Hindawi
Journal of Nanomaterials
Volume 2023, Article ID 4235308, 15 pages
https://doi.org/10.1155/2023/4235308

Research Article

Assessment on the Toxic Effects of Chemically Synthesized SPIONs against Model Organisms

Chellapan Justin,[1] Antony V. Samrot,[2] Nagarajan Shobana,[1] Mahendran Sathiyasree,[1] Subramanian Saigeetha,[3] Rajan Renuka Remya,[4] Deenadhayalan Rajalakshmi,[1] and S. Prasath[5]

[1]*Department of Biotechnology, School of Bio and Chemical Engineering, Sathyabama Institute of Science and Technology, Chennai 600119, Tamil Nadu, India*
[2]*School of Bioscience, Faculty of Medicine, Bioscience and Nursing, MAHSA University, Jalan SP2, Bandar Saujana Putra, Jenjarom 42610, Selangor, Malaysia*
[3]*Department of Biotechnology, School of Biosciences and Technology, Vellore Institute of Technology, Vellore 632014, Tamil Nadu, India*
[4]*Centre for Materials Engineering and Regenerative Medicine, Bharath Institute of Higher Education and Research, Chennai 600073, Tamil Nadu, India*
[5]*Department of Mechanical Engineering, College of Engineering and Technology, Mizan Tepi University, Mizan Teferi, Ethiopia*

Correspondence should be addressed to Antony V. Samrot; drantonysamrot@gmail.com and S. Prasath; prasath@mtu.edu.et

Received 17 April 2022; Revised 14 June 2022; Accepted 24 April 2023; Published 19 September 2023

Academic Editor: Hiwa M. Ahmed

The remarkable physicochemical properties of nanomaterials have attracted researchers due to the numerous applications in the field of chemistry, biology, and physics. Despite the various applications, superparamagnetic iron oxide nanoparticles (SPIONs) are harmful to living organisms and to the environment as they are released without any safety testing. In this study, SPIONs were synthesized and further characterized. The aim of the study was to examine the toxicity of synthesized SPIONs against animal models: Zebrafish—*Danio rerio*, Earthworm—*Eudrilus eugeniae*, and Drosophila—*Drosophila melanogaster* through histology using Hematoxylin–Eosin and Prussian Blue staining. The accumulation of SPIONs was further quantified by using Inductively Coupled Plasma Mass Spectrometry (ICP-MS). Through histology images, it was observed that the SPIONs had caused damages and a lower concentration of 0.001–0.002 μg/ml of metal accumulation was detected in the ICP-MS analysis.

1. Introduction

New horizons of technical advancement have been opened with the help of nanotechnology [1]. There are some promising applications of nanoparticles in nanomedicine, wastewater treatment, etc. [2–7]. Magnetism is one of the numerous magnificent qualities of nanoparticles that fascinates researchers of both material sciences and biosciences [8–10]. Research is being conducted on the applications of magnetic nanoparticles in many fields [11–14], which include improving cell seeding and distribution in tissue engineering scaffolds, targeted imaging, and therapy [15, 16]; targeted imaging and therapy [17]; improving anticancer drug efficiency by amplifying reactive oxygen species stress [18]; drug delivery applications [13]; magnetic resonance imaging [19]; magnetically induced local hyperthermia [20–22]; wastewater treatment [23–30], etc. Superparamagnetic Iron Oxide Nanoparticles (SPIONs) act as carriers for drug targets as they obey to an external magnetic field [31]. They can deliver biotherapeutics by targeting the ligands or stimulator-sensitive moieties that are responsive to external stimuli, such as light, ultrasounds, or magnetic fields [32]. They help in the implementation of drugs directly to the target area with lower systemic concentration [33]. SPIONs are also employed in the diagnosis of a variety of diseases. Intravenous injection of folate-tagged SPIONs in an antigen-induced arthritis model improved macrophage

Table 1: Dietary ratio provided to *Danio rerio*.

Organism	Feed	Ratio of feed (1)	Ratio of feed (2)	Ratio of feed (3)	Ratio of feed (4)	Control
Danio rerio	NP : NF	1 : 3	2 : 2	3 : 1	4 : 0	0 : 4

NPs - Nanoparticles; NF - Normal Feed.

Table 2: Dietary ratio provided to *Eudrilus eugeniae*.

Organism	Feed	Ratio of feed (1)	Ratio of feed (2)	Ratio of feed (3)	Ratio of feed (4)	Control
Eudrilus eugeniae	NP : NF	1 : 3	2 : 2	3 : 1	4 : 0	0 : 4

NPs - Nanoparticles; NF - Normal Feed.

Table 3: Dietary ratio provided to *Drosophila melanogaster*.

Organism	Feed	Ratio of feed (1)	Ratio of feed (2)	Ratio of feed (3)	Ratio of feed (4)	Control	Generation
Drosophila melanogaster	NP : NF	0.002 ml : 50 ml	0.003 ml : 50 ml	0.004 ml : 50 ml	0.005 ml : 50 ml	50 ml of feed without NPs	3

NPs - Nanoparticles; NF - Normal Feed.

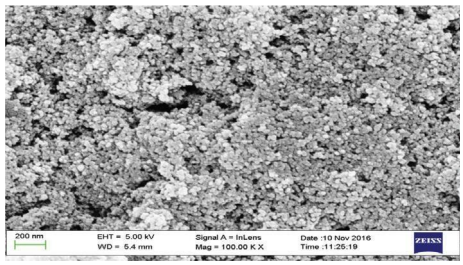

Figure 1: SEM analysis of SPIONs.

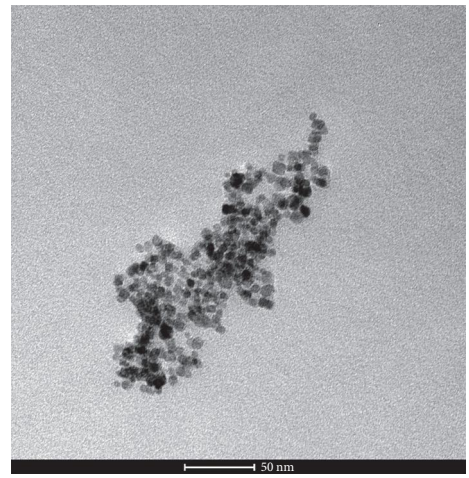

Figure 2: TEM analysis of SPIONs.

endocytosis *in vitro* and produced hypointense signals in affected joints; it may also be used in X-ray imaging [34, 35].

Despite the advantages, biocompatibilities and toxicities of iron oxide nanoparticles raise real concerns [36, 37]. When iron oxide nanoparticles were injected into a rat model, it was claimed that they created oxidative stress, lowering the antioxidant capability of the blood cells [38, 39]. It has been reported that nanoparticles induce oxidative stress, which affects cell signaling [40]. SPIONs are reported to cause oxidative stress responses such as inflammation, damage to the membrane, denaturation of protein, mitochondria-mediated apoptosis, lipid peroxidation, genotoxicity, etc. [41, 42]. Low level of oxidative stress activates the genes responsible for transcription defense through transcription factor, leading to the activation of inflammation and apoptosis, and necrosis [43]. The impact of iron oxide nanoparticles on cellular systems, like vascular systems, including blood cells, fibroblast, stromal cells, reproductive cells, lung cells, liver cells, kidney cells, and cerebral cells, have also been reported earlier [44]. Iron oxide nanoparticles induces genotoxicity in intratracheally instilled mouse lungs, and the inflammatory responses lead to oxidative and lipid peroxide-related DNA adduct formations [45–48]. The CCK-8 and lactate dehydrogenase assays can be used to determine cytotoxicity [49], and Comet reaction can be used to determine the genotoxicity in biological tissue [50]. Various functional groups can be added to SPIONs to minimize the adverse biological effects [51]. Mice, Drosophila [46], earthworms [52], fishes [53–56], and even its embryos [36, 57] are some of the model organisms previously reported for studying the toxicological effects of iron oxide nanoparticles. The objective of this investigation is to explore the histopathological impact of SPIONs in three different animal models: zebrafish (*Danio rerio*), earthworms (*Eudrilus eugeniae*), and Drosophila (*Drosophila melanogaster*). The study aims to assess the harm and accumulation of SPIONs resulting from their administration to these animal models. This research provides insights into the potential applications of SPIONs in fields such as drug delivery and X-ray imaging.

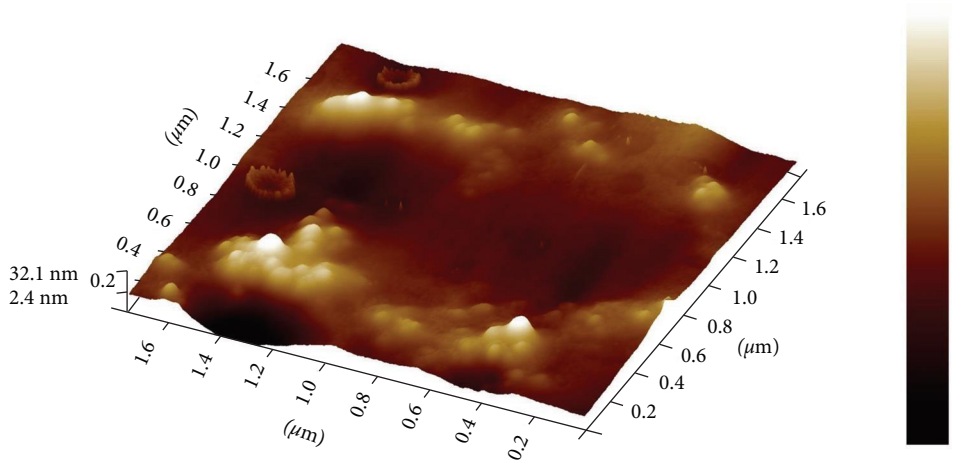

Figure 3: AFM analysis of SPIONs.

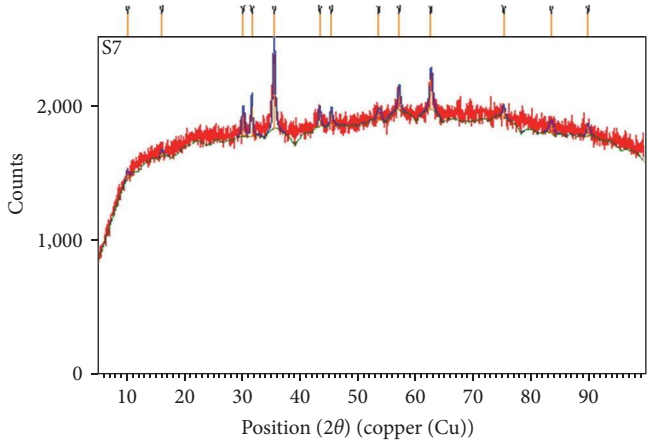

Figure 4: XRD analysis of SPIONs.

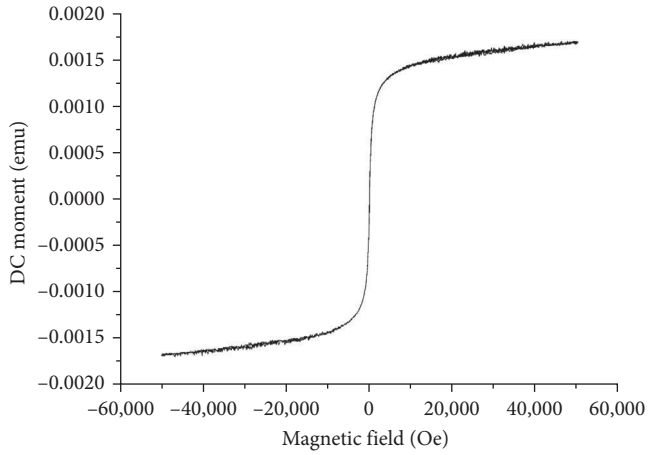

Figure 5: VSM analysis of SPIONs.

Previous studies have demonstrated that SPIONs with varying physiochemical properties can exhibit either lower cytotoxicity or toxicity that is dependent on the dosage, particularly at dosages of 100 g/ml or higher [58].

2. Materials and Methods

2.1. Materials Required. Ferrous sulfate heptahydrate ($FeSO_4{\cdot}7H_2O$) was purchased from HiMedia; Ferric chloride hexahydrate ($FeCl_3{\cdot}6H_2O$) from Thomas Baker; Formaldehyde (CH_2O) and tetramethylammonium hydroxide ($C_4H_{13}NO$) from SD Fine-Chem Limited, Mumbai, India, and agar from Micro Fine Chemicals. Semolina was acquired from Vedant Organics (div. of Esteem Pharmaceuticals); jaggery from Cloudtail India. Zebrafishs (*D. rerio*) were procured from Aquarium Professionals; earthworms (*E. eugeniae*) from SS Vermicompost and Drosophila (*D. melanogaster*) from The Genetics Laboratory of Kristu Jayanti College, Bengaluru, India.

2.2. Synthesis of SPIONs. SPIONs were synthesized using magnetic field-mediated reaction method [35]. Accordingly, 0.1 g of ferric chloride hexahydrate ($FeCl_3{\cdot}6H_2O$) and 0.1 g of ferrous sulfate heptahydrate ($FeSO_4{\cdot}7H_2O$) were separately dissolved in 1 ml of nitrogenized double distilled water and then mixed together for 5 min. 500 µl of nitrogenized iron salt solution was then added to 500 μl of tetramethylammonium hydroxide ($C_4H_{13}NO$) and kept in vortex for 5 min. The obtained black precipitate was then washed in 1 ml of acetone and dried in hot air oven at 60°C for 30 min. The pellet was then dissolved in 700 μl of formaldehyde solution (CH_2O), and 300 μl of nitrogenized H_2O was added dropwise with simultaneous vortex, which was followed by 500 μl formaldehyde solution. The obtained solution was then kept in the magnetic field for 2 days and was then dispersed in formaldehyde solution. The nanoparticles were then washed four to five times in nitrogen-purged double distilled water prior to toxicological experiments.

2.3. Characterization of SPIONs. Characterization of SPIONs was done to analyze their chemical and structural properties. The SPIONs were subjected to Scanning Electron Microscopy (SEM) (Zeiss Ultra Plus, Oberkochen, Germany), Transmission Electron Microscopy (TEM) (TEECNAI G2 Spirit Biotwin—120 kV), where the size and surface morphology of synthesized SPIONs were checked, Atomic Force Microscopy (AFM)

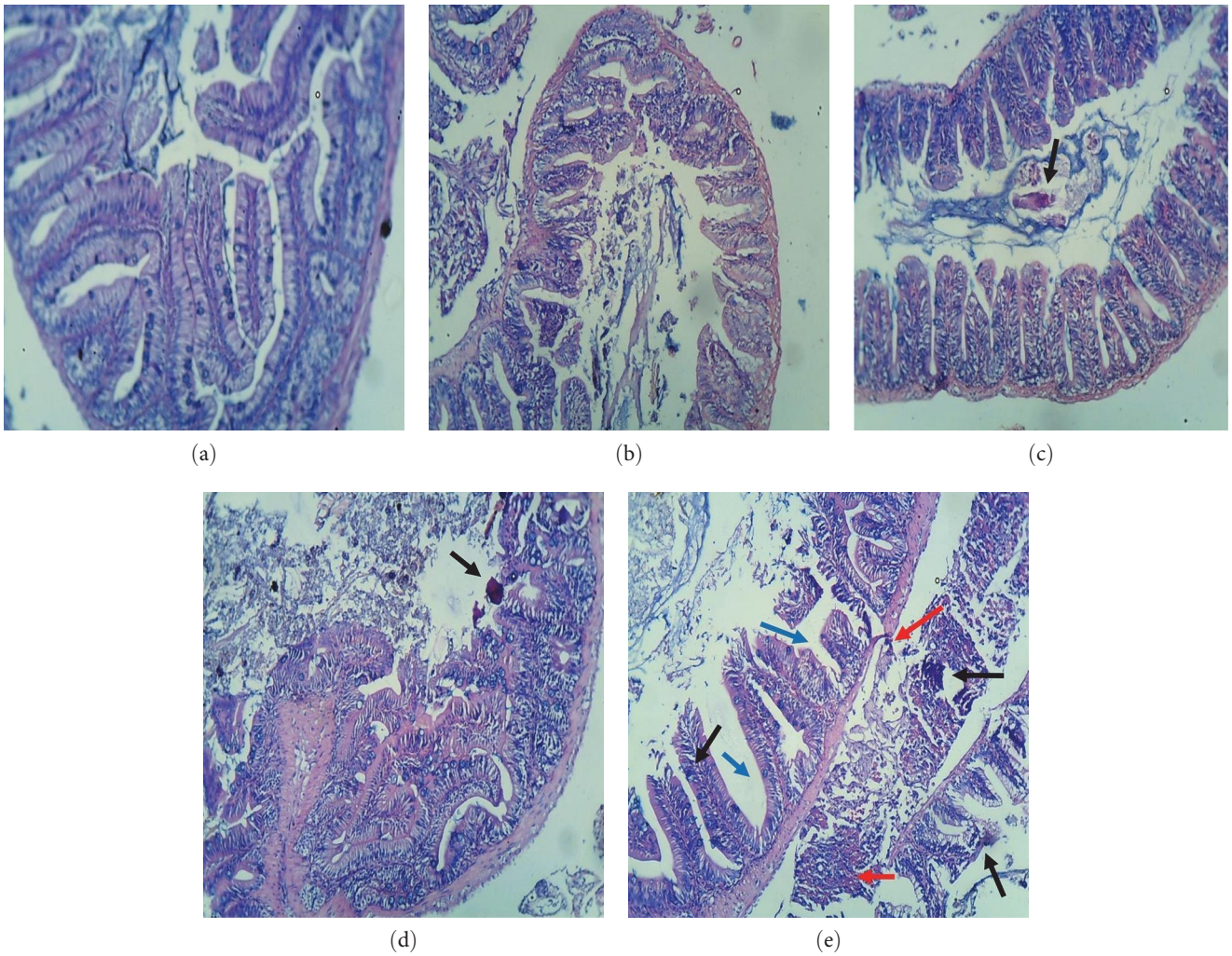

Figure 6: Histology images of zebrafish exposed to different concentrations of SPIONs using Hematoxylin–Eosin stain: (a) control; (b) 1 : 3 ratio of SPIONs to feed; (c) 2 : 2 ratio of SPIONs to feed; (d) 3 : 1 ratio of SPIONs to feed; (e) 4 : 0 ratio of SPIONs to feed. Black arrow lipofuscin; red arrow erosion of organ; blue arrow interstitial space.

(Bruker, Dimension icon model, Germany) to examine the confinement of the nanoparticle to the three coordinates as 3D images, X-ray Diffraction (XRD) by Smartlab X-ray Diffractometer (Rigaku Corporation, Japan) to check the crystallinity and Vibrating Sample Magnetometer (VSM) (LakeShore Co. Ltd., Lake Shore 7407, Westerville, Ohio, USA) with a maximum magnetic field of 2.5 T and dynamic moment range of $1 \times 10e^{-6}$–$10e^{3}$ emu to check the magnetization property.

2.4. Feed Preparation. Feed was prepared separately for *D. rerio*, *E. eugeniae*, and *D. melanogaster*. Stock solution of 0.010 mg/10 ml of SPIONs were prepared using distilled water and used in this study against earthworm and zebrafish. For study against *Drosophila*, we used different concentrations of SPIONs ranging from 0.002 g/1 ml to 0.005 g/1 ml.

2.4.1. D. rerio Feed Preparation. Micro pellet feed was soaked in different concentrations of SPIONs suspension and incubated at room temperature until all the nanoparticles were absorbed into the feed. It was then dried in a hot air oven at 40°C overnight, after which the nanoabsorbed feed was kept at the room temperature for 15 min to cool and then stored for further use.

2.4.2. E. eugeniae Feed Preparation. Dried cow dung was fed to the *E. eugeniae*. The stock SPIONs solution was suspended in the deionized water in different concentrations and were sprayed onto the cow dung and dried, which was then stored for further use.

2.4.3. D. melanogaster Feed Preparation. 25 g of jaggery was crushed and boiled in 250 ml of water until it was dissolved completely. 25 g of semolina was added to the previously prepared solution, which was followed by the addition of 10% agar. About 1.9 ml of propionic acid was added to the prepared porridge and thoroughly stirred while it was still hot. The porridge was then transferred to 5 beakers (50 ml each). Stock SPIONs of varied concentrations were added to the heated mixture and thoroughly stirred. 10 ml of each was poured into separate test tubes while the porridge was still

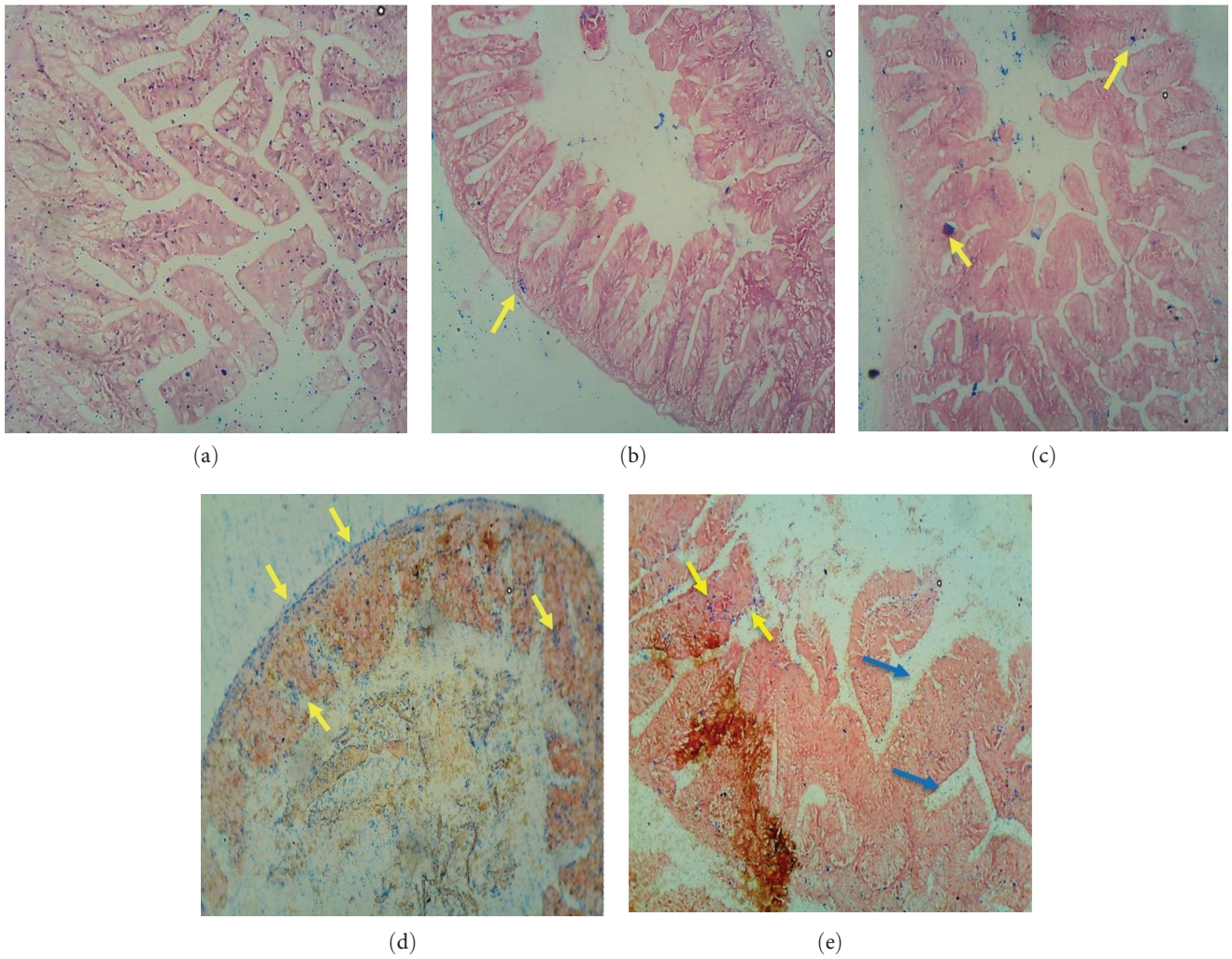

Figure 7: Histology images of zebrafish exposed to different concentrations of SPIONs using Prussian Blue stain: (a) control; (b) 1 : 3 ratio of SPIONs to feed; (c) 2 : 2 ratio of SPIONs to feed; (d) 3 : 1 ratio of SPIONs to feed; (e) 4 : 0 ratio of SPIONs to feed. Black arrow lipofuscin; blue arrow interstitial space; yellow arrow denotes iron accumulation.

warm. After 10 min, the moisture content in the test tubes was wiped with cotton and kept overnight for solidification.

2.5. Feeding the Organisms. Four different concentrations of feed were given to *D. rerio*, *E. eugeniae*, and *D. melanogaster*.

2.5.1. Feeding D. rerio. After a month-long acclimation, *D. rerio* were bifurcated into five different fish bowls, among which one bowl was considered as control. The administered feed details are given in Table 1.

2.5.2. Feeding E. eugeniae. E. eugeniae were introduced to the soil containing cow dung in a plastic tub and allowed to acclimate for a week. The earthworms were fed dried cow dung at regular intervals. In order to ensure proper growing circumstances for the earthworms, the moisture conditions in the box were also checked regularly. The administered feed details are given in Table 2.

2.5.3. Feeding D. melanogaster Culture. D. melanogaster (10 flies each) were inoculated into the prepared test tubes for feeding and the study for three generations, i.e., larva, pupa, and adult fly, each of which were collected for analysis. The administered feed details are given in Table 3.

2.6. Inductively Coupled Plasma Mass Spectrometry (ICP-MS) and Staining of Organisms. The organisms after the study period, were subjected to histopathological staining, for which they were preserved in 10% formaldehyde solution. Hematoxylin–Eosin (H&E) staining was done to detect changes in the tissue of the organism, according to the procedure followed by Samrot et al. [59] and Cardiff et al. [60]. Prussian Blue staining was also done to examine the iron accumulation inside the tissue [61–63]. Organisms from each concentration were subjected to acid digestion [64] and analyzed using ICP-MS analysis (Agilent Technologies, 7700 series, Santa Clara, CA, USA).

3. Results and Discussion

3.1. Characterization of SPIONS. The topographical view revealed that the size of synthesized SPIONs was in the range

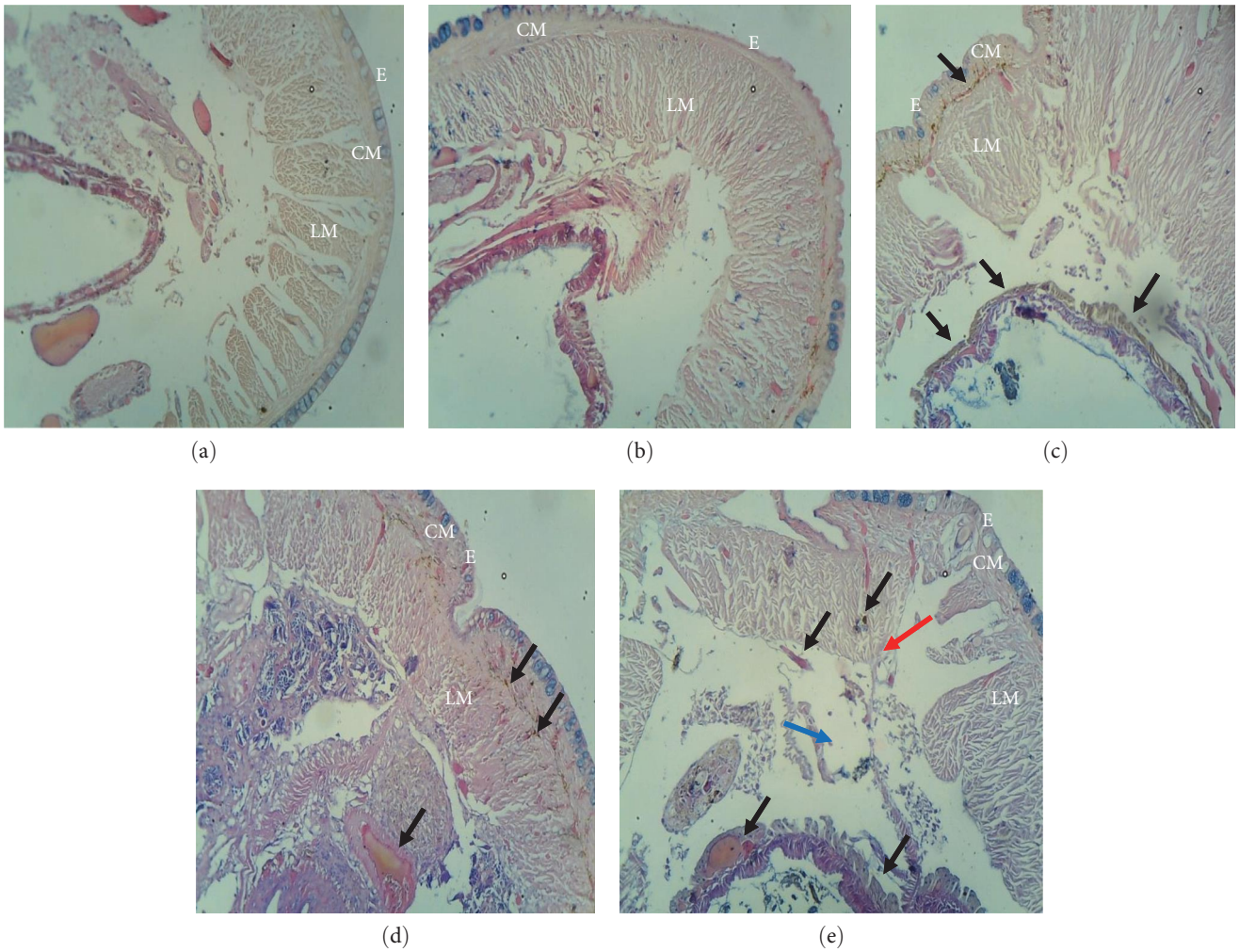

Figure 8: Histology images of earthworms exposed to different concentrations of SPIONs using Hematoxylin–Eosin stain: (a) control; (b) 1 : 3 ratio of SPIONs to feed; (c) 2 : 2 ratio of SPIONs to feed; (d) 3 : 1 ratio of SPIONs to feed; (e) 4 : 0 ratio of SPIONs to feed. Black arrow lipofuscin; red arrow erosion of organ; blue arrow interstitial space. E, Epidermis; CM, Circular Muscle; LM, Longitudinal Muscle.

10–25 nm (Figure 1), which was also confirmed by TEM images (Figure 2). Samrot et al. [59] also reported the size of SPIONs to be around 25 nm, synthesized using ammonia as a reducing agent. In earlier reports, Samrot et al. [65] synthesized SPIONs which ranged from 9 to 25 nm. SPIONs synthesized using precursor solutions such as $FeCl_3$ and $FeCl_2$ were found to be 40–45 nm in size [66]. In a study by Sathya et al. [67], the size of iron oxide nanoparticles synthesized using a magnetic stirrer and ultrasound method ranged from 20 to 90 nm.

The 3D structure of the synthesized SPIONs was confirmed by AFM analysis (Figure 3). It was confirmed that the particles were spherical and well dispersed. According to the XRD pattern (Figure 4), the synthesized SPIONs were in the inverse spinel structure. Shukla et al. [68] reported that the iron oxide nanoparticles exhibited peaks at 30.1, 35.5, 42.6, 53.6, 57.0, and 62.8 assigned to the diffraction plane of the spinel structured magnetite nanoparticles (220), (311), (400), (422), (511), and (440), respectively. VSM measurements were done to estimate the magnetization and coercivity of the synthesized SPIONs. The magnetization curves clearly indicated the superparamagnetic behavior of the synthesized SPIONs (Figure 5).

3.2. Histology. H&E stain is usually used for the identification of different kinds of cells and its pattern, shape, and structures, whereas Prussian Blue staining is performed to identify the accumulation of iron as it can form ferric ferrocyanide complex by producing blue color in the tissue [69, 70]. Intestines of *D. rerio* were stained using H&E following exposure to different concentrations of SPIONs (Figure 6). Lower concentrations of SPIONs did not show any significant impact, whereas exposure of higher concentrations caused erosion in the goblet cells in the intestinal area and on the intestinal wall of *D. rerio*. Tissues stained using Prussian Blue (Figure 7) revealed the accumulation of iron oxide nanoparticles inside the tissues. It was accumulated in and around the intestinal walls. Samrot et al. [59] earlier reported that the metal nanoparticles impacted the rate of reproduction.

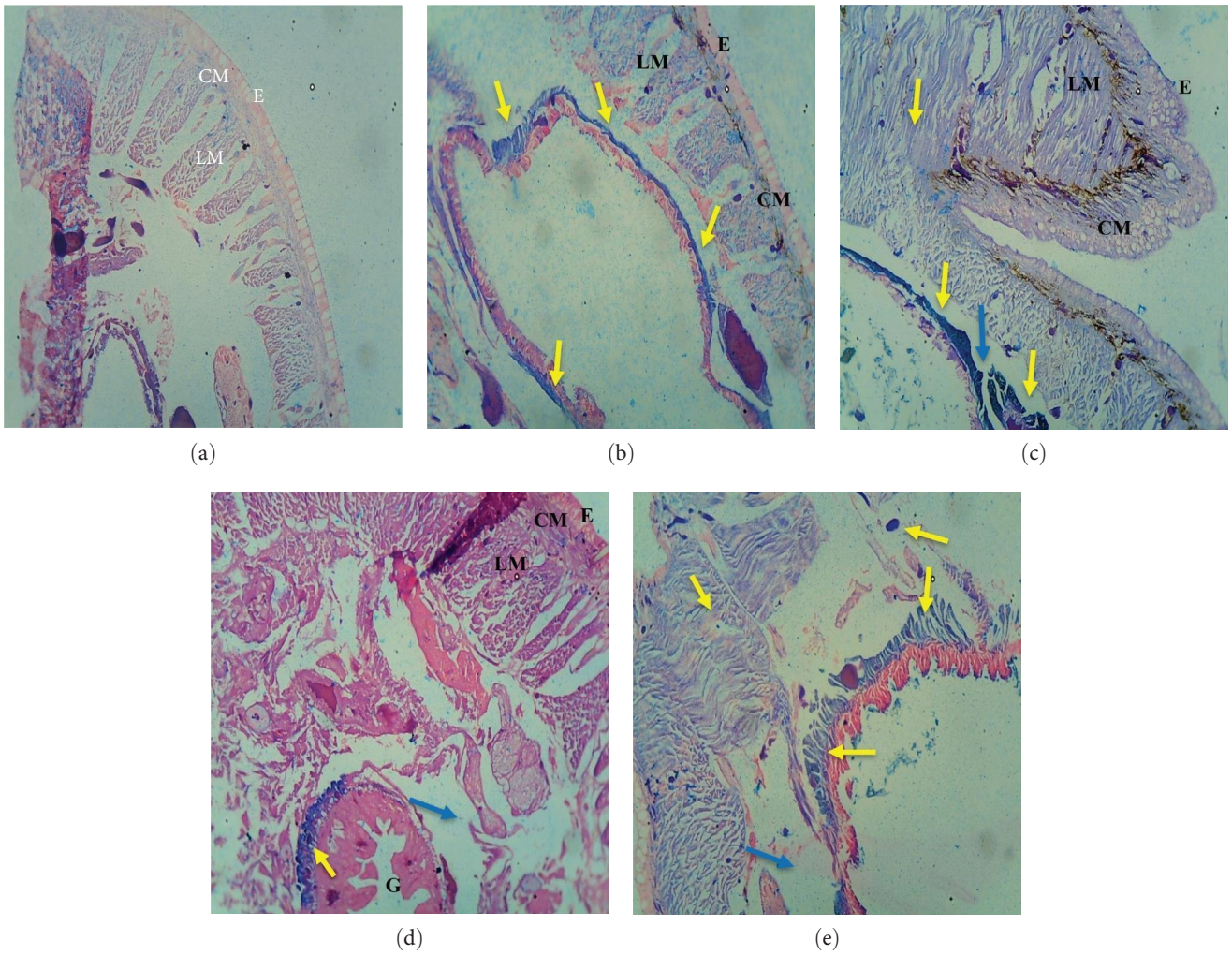

Figure 9: Histology images of earthworms exposed to different concentrations of SPIONs using Prussian Blue stain: (a) control; (b) 1 : 3 ratio of SPIONs to feed; (c) 2 : 2 ratio of SPIONs to feed; (d) 3 : 1 ratio of SPIONs to feed; (e) 4 : 0 ratio of SPIONs to feed. Black arrow lipofuscin; blue arrow interstitial space; yellow arrow denotes iron accumulation. G, Gut; E, Epidermis; CM, Circular Muscle; LM, Longitudinal Muscle.

Villacis et al. [71] reported the occurrence of fragmentation of DNA and micronuclei, malondialdehyde generation, and reduction in gene expression.

The exposure of SPIONs had a negative impact on the tissue of *E. eugeniae* as well, which was seen in the histology images. The earthworm's exterior structure was altered significantly. As the concentration of SPIONs increased, the circular and longitudinal muscles were found to be degraded in addition to the gizzard area (Figure 8). *E. eugeniae* treated with different concentrations of SPIONs, and control were also studied using Prussian Blue staining (Figure 9), which showed the accumulation of SPIONs and is believed to be the reason for damaged circular muscle and epidermal erosion. In earlier reports, it has been evidenced that exposure of Fe_2O_3 onto the earthworm, significantly decreased its growth and rate of reproduction [72, 73]. Samrot et al. [52] also reported erosion of epithelium, fibrosis of the circular muscle, and gut disintegration of earthworms on exposure to magnetite nanoparticles.

The histology images of *D. melanogaster* exposed to different concentrations of SPIONs. Figures 10–15 depicted visible distortion in the waxy cuticles of larvae at lower concentrations, whereas degradation at higher concentrations was also noticed (Figure 10). The deposition of iron in the larvae of *D. melanogaster* in Figure 11 is visualized using Prussian Blue staining. The images show the accumulation of SPIONs in the larvae's anterior and in the midguts. The mouth, spiracles, and trachea in the anterior and the ovary and gonads in the posterior of the larvae have been found to be degraded at higher concentrations.

The histology images of the *D. melanogaster* pupa stained with H&E are shown in Figure 12. The images do not show any damages after being exposed to lower concentrations, such as 0.002 g : 50 ml and 0.003 g : 50 ml of SPIONs : feed ratio but higher concentrations, such as 0.004 g : 50 ml and 0.005 g : 50 ml, exhibited erosion of the puparium, anterior, and posterior regions and severe damages in the tracheal region. The Prussian Blue staining of the pupa illustrated the accumulation of the iron

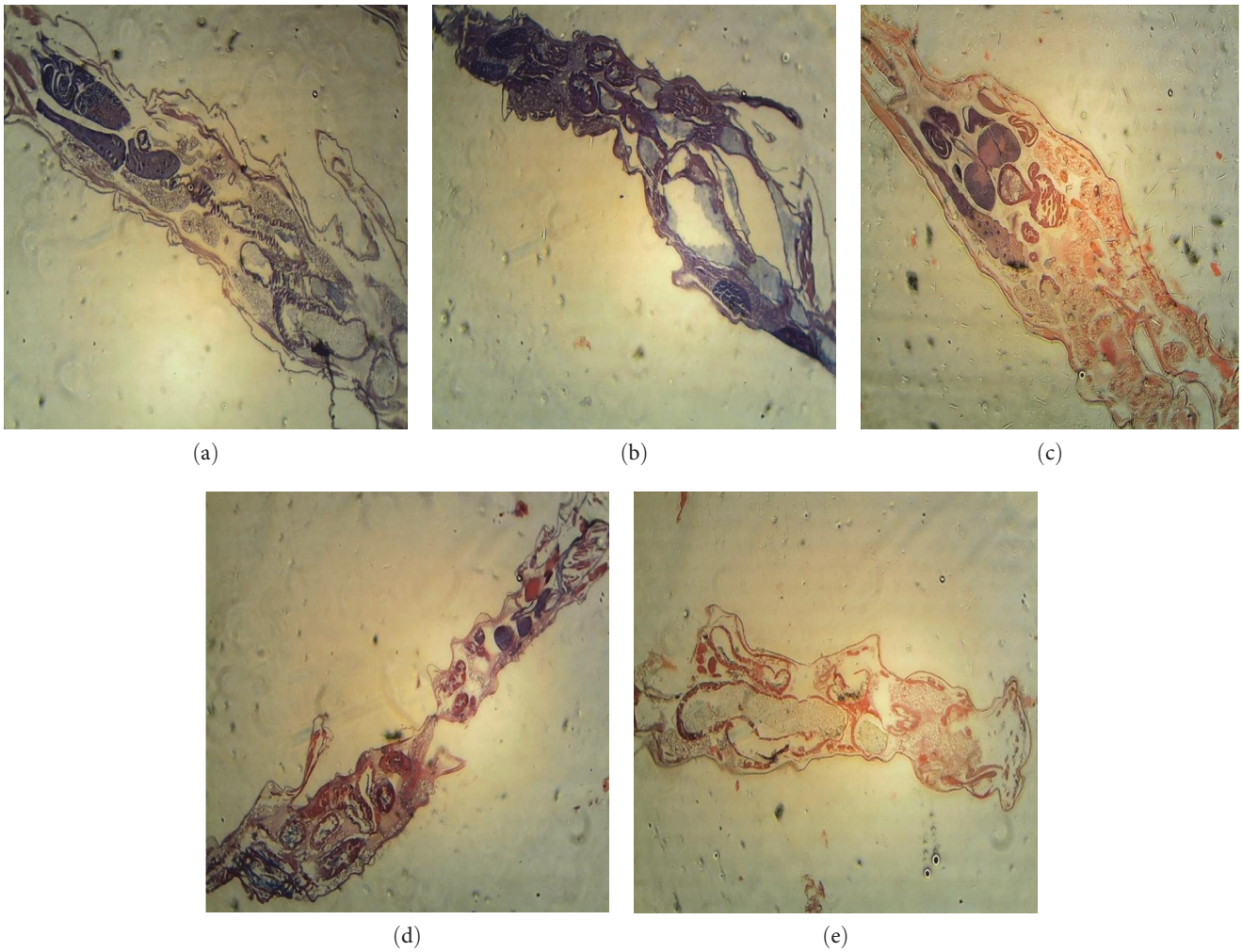

(a) (b) (c)

(d) (e)

Figure 10: Histology images of Drosophila larva exposed to different concentrations of SPIONs using Hematoxylin–Eosin stain: (a) Control; (b) 0.002 g : 50 ml ratio of SPIONs to feed; (c) 0.003 g : 50 ml ratio of SPIONs to feed; (d) 0.004 g : 50 ml ratio of SPIONs to feed; (e) 0.005 g : 50 ml ratio of SPIONs to feed.

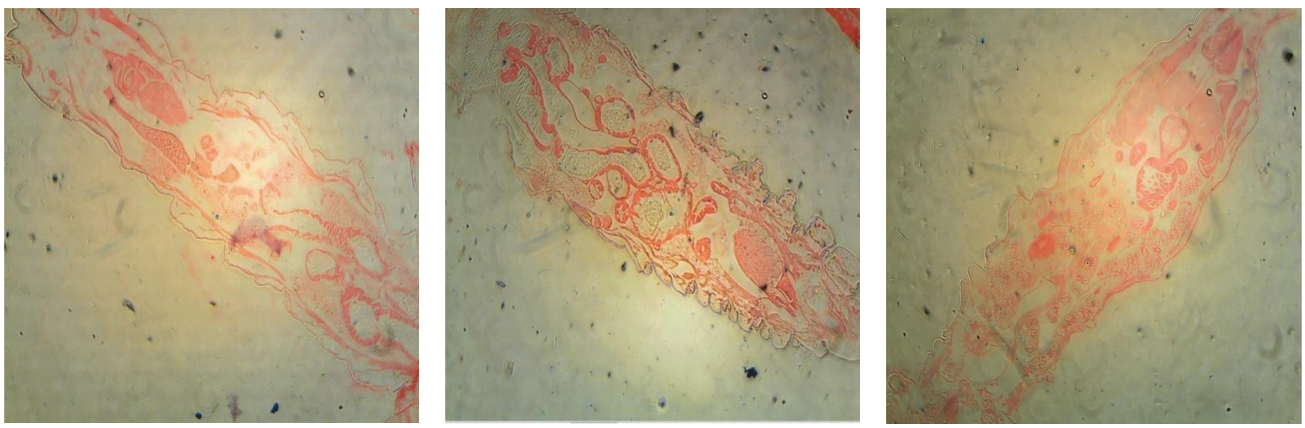

(a) (b) (c)

Figure 11: Continued.

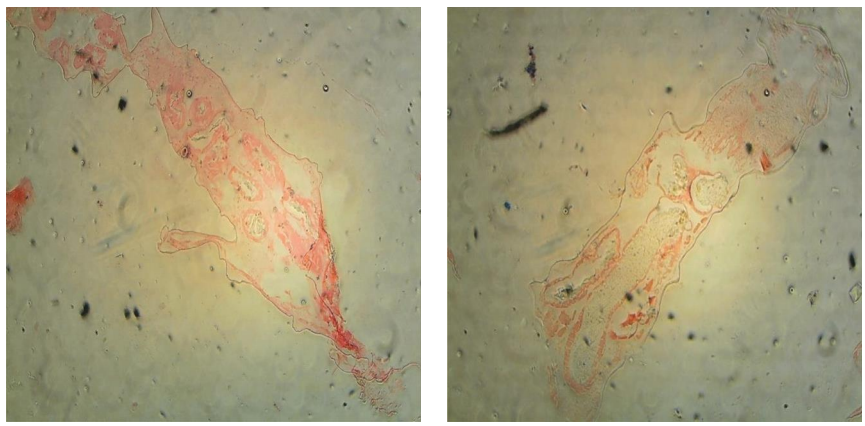

(d) (e)

Figure 11: Histology images of Drosophila larva exposed to different concentrations of SPIONs using Prussian Blue stain: (a) control; (b) 0.002 g : 50 ml ratio of SPIONs to feed; (c) 0.003 g : 50 ml ratio of SPIONs to feed; (d) 0.004 g : 50 ml ratio of SPIONs to feed; (e) 0.005 g : 50 ml ratio of SPIONs to feed.

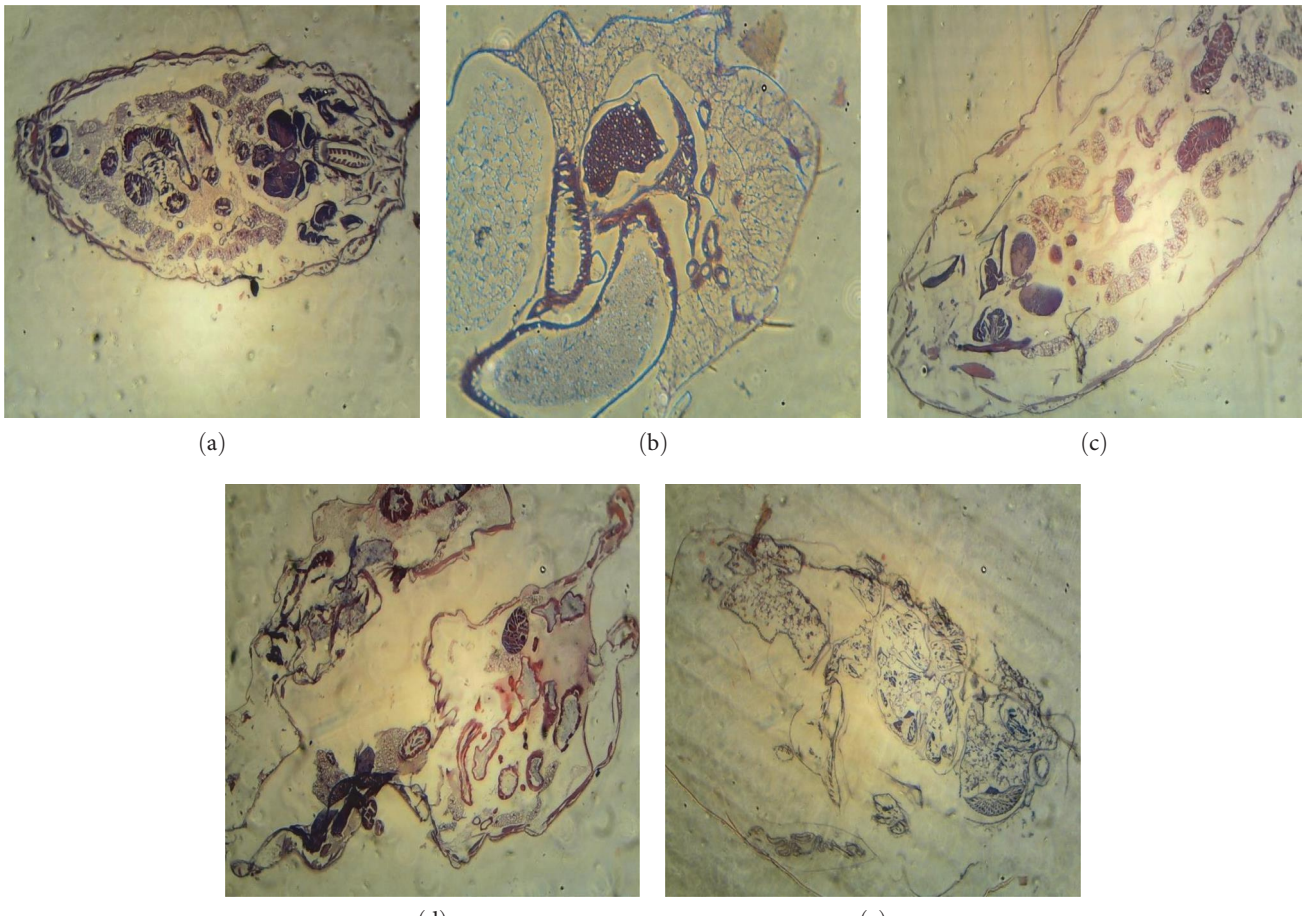

(a) (b) (c)

(d) (e)

Figure 12: Histology images of Drosophila pupa exposed to different concentrations of SPIONs using Hematoxylin–Eosin stain: (a) control; (b) 0.002 g : 50 ml ratio of SPIONs to feed; (c) 0.003 g : 50 ml ratio of SPIONs to feed; (d) 0.004 g : 50 ml ratio of SPIONs to feed; (e) 0.005 g : 50 ml ratio of SPIONs to feed.

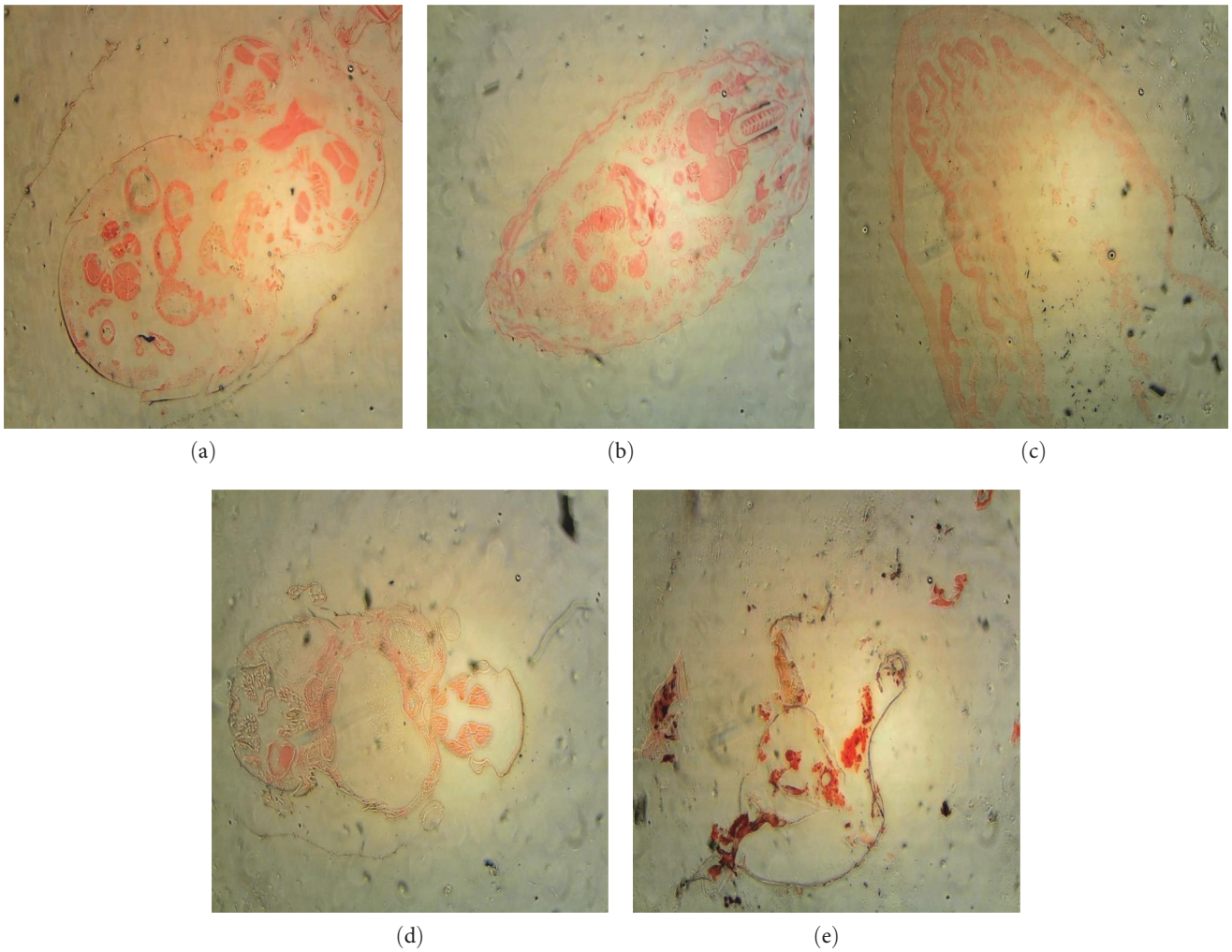

(a) (b) (c)

(d) (e)

Figure 13: Histology images of Drosophila pupa exposed to different concentrations of SPIONs using Prussian Blue stain: (a) control; (b) 0.002 g : 50 ml ratio of SPIONs to feed; (c) 0.003 g : 50 ml ratio of SPIONs to feed; (d) 0.004 g : 50 ml ratio of SPIONs to feed; (e) 0.005 g : 50 ml ratio of SPIONs to feed.

(a) (b) (c)

Figure 14: Continued.

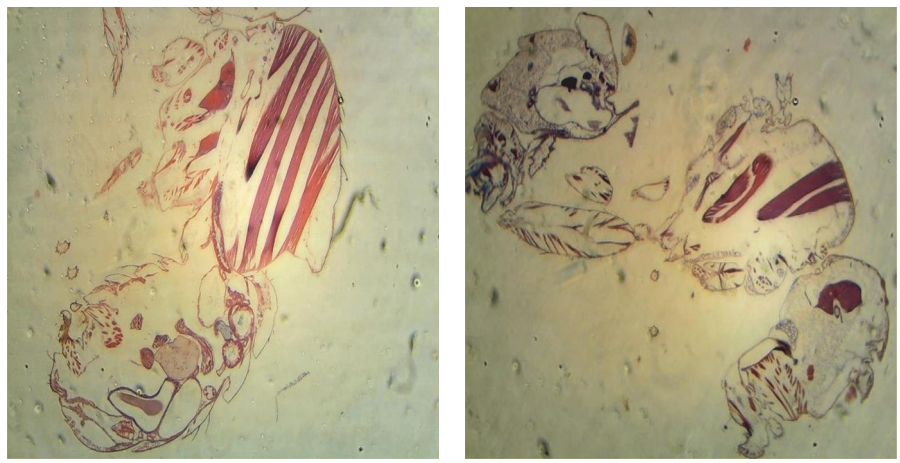

(d) (e)

Figure 14: Histology images of adult Drosophila exposed to different concentrations of SPIONs using Hematoxylin–Eosin stain: (a) control; (b) 0.002 g : 50 ml ratio of SPIONs to feed; (c) 0.003 g : 50 ml ratio of SPIONs to feed; (d) 0.004 g : 50 ml ratio of SPIONs to feed; (e) 0.005 g : 50 ml ratio of SPIONs to feed.

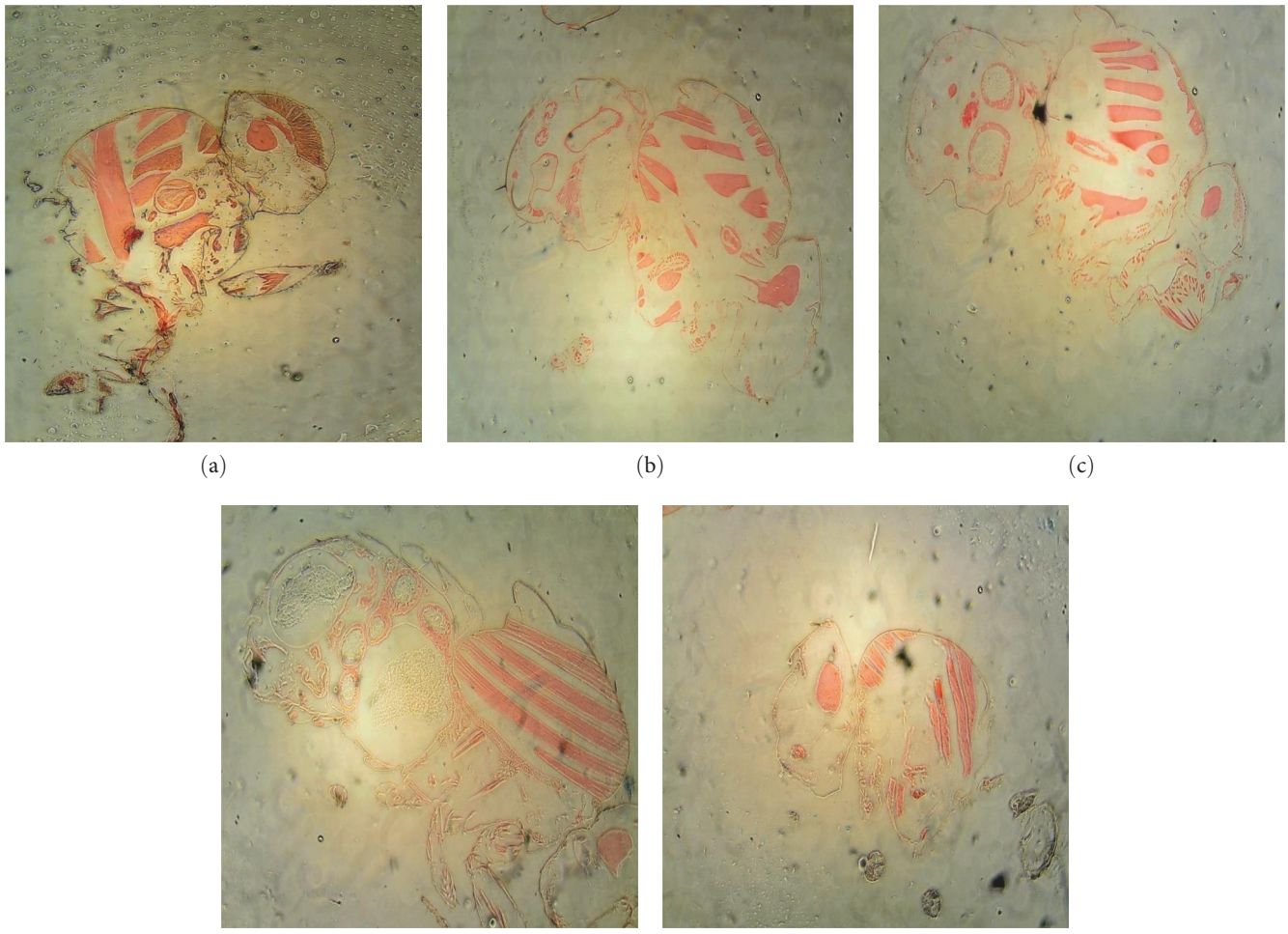

(a) (b) (c)

(d) (e)

Figure 15: Histology images of adult Drosophila exposed to different concentrations of SPIONs using Prussian Blue stain: (a) control; (b) 0.002 g : 50 ml ratio of SPIONs to feed; (c) 0.003 g : 50 ml ratio of SPIONs to feed; (d) 0.004 g : 50 ml ratio of SPIONs to feed; (e) 0.005 g : 50 ml ratio of SPIONs to feed.

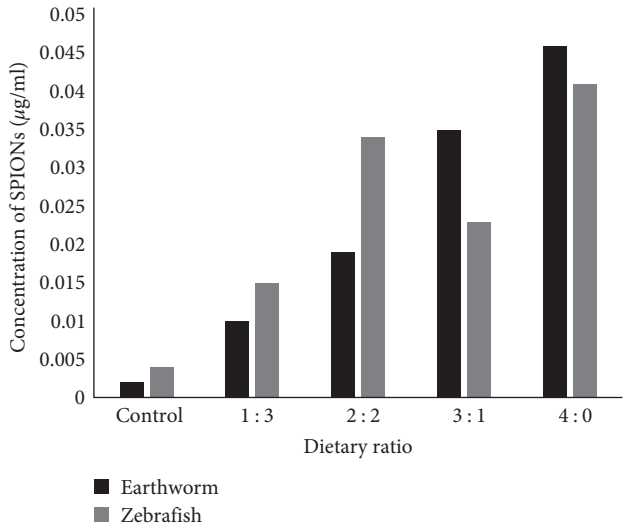

Figure 16: ICP-MS analysis for earthworms and zebrafish.

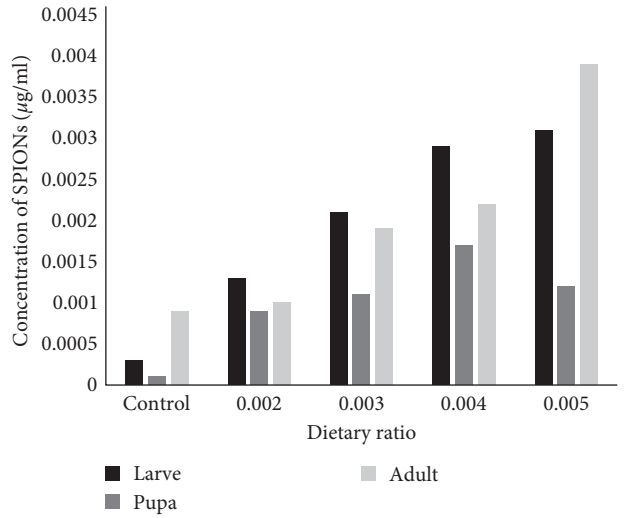

Figure 17: ICP-MS analysis for different stages of Drosophila.

(Figure 13). No visible accumulations were observed at lower concentrations, but at higher concentrations, the posterior region of pupa was accumulated with iron nanoparticles. Raj et al. [74] reported that a high dose of silver nanoparticles at the early stages of development could negatively impact the behavior and metabolism of *D. melanogaster*.

Adult *D. melanogaster* did not show any considerable impact at the lower concentration but revealed the formation of lipofuscin-like granules in the abdominal region. But whereas at higher concentrations, the head, thorax, and abdomen were entirely distorted (Figure 14). The iron accumulation is visible in the histology images (Figure 15) stained by Prussian Blue. Abdominal region of adult *D. melanogaster* also showed lipofuscin-like granules responsible for the erosion in gut area. The thorax and abdomen were entirely degraded at the higher concentrations. Ong [75] revealed that the survival rate of *D. melanogaster* fed with silver nanoparticles decreased significantly when compared to control flies.

3.3. ICP-MS Analysis. The concentration of SPIONs in the aqueous solution of acid-digested organisms from each concentration was studied using ICP-MS analysis [76]. The control samples showed no substantial deposition, albeit a small amount (0.001–0.002 μg/ml) was detected, which can be attributed to the presence of metal in the organism's natural habitat. Figures 16 and 17 shows the metal accumulation inside the bodies of *D. rerio*, *E. eugeniae*, and different stages of *D. melanogaster*, which was supported by histology images as well.

4. Conclusion

SPIONs have been synthesized and characterized using SEM, TEM, AFM, XRD, and VSM in this study. The toxicity studies of SPIONs were carried against *D. rerio*, *E. eugeniae*, and the different stages of *D. melanogaster* and histology studies were carried out by staining the tissues with H&E and Prussian Blue. The exposure of nanoparticles onto the organisms were depicted through histology studies, and metal accumulation was investigated by ICP-MS analysis. The synthesized SPIONs had considerable damages in the organisms which are suspected to be toxic.

Data Availability

The data used to support the findings of this study are included within the article.

Conflicts of Interest

The authors declare that they have no conflicts of interest.

References

[1] C. C. Fleischer and C. K. Payne, "Nanoparticle surface charge mediates the cellular receptors used by protein–nanoparticle complexes," *The Journal of Physical Chemistry B*, vol. 116, no. 30, pp. 8901–8907, 2012.

[2] Y.-M. Chu, U. Nazir, M. Sohail, M. M. Selim, and J.-R. Lee, "Enhancement in thermal energy and solute particles using hybrid nanoparticles by engaging activation energy and chemical reaction over a parabolic surface via finite element approach," *Fractal and Fractional*, vol. 5, no. 3, Article ID 119, 2021.

[3] Y.-M. Chu, B. M. Shankaralingappa, B. J. Gireesha, F. Alzahrani, M. Ijaz Khan, and S. U. Khan, "Combined impact of Cattaneo-Christov double diffusion and radiative heat flux on bio-convective flow of Maxwell liquid configured by a stretched nano-material surface," *Applied Mathematics and Computation*, vol. 419, Article ID 126883, 2022.

[4] B. Hayati, N. M. Mahmoodi, and A. Maleki, "Dendrimer–titania nanocomposite: synthesis and dye-removal capacity," *Research on Chemical Intermediates*, vol. 41, pp. 3743–3757, 2015.

[5] N. M. Mahmoodi, "Synthesis of magnetic carbon nanotube and photocatalytic dye degradation ability," *Environmental Monitoring and Assessment*, vol. 186, pp. 5595–5604, 2014.

[6] N. M. Mahmoodi, S. Keshavarzi, and M. Ghezelbash, "Synthesis of nanoparticle and modelling of its photocatalytic dye degradation ability from colored wastewater," *Journal of Environmental Chemical Engineering*, vol. 5, no. 4, pp. 3684–3689, 2017.

[7] N. M. Mahmoodi and M. H. Saffar-Dastgerdi, "Clean Laccase immobilized nanobiocatalysts (graphene oxide–zeolite nanocomposites): from production to detailed biocatalytic degradation of organic pollutant," *Applied Catalysis B: Environmental*, vol. 268, Article ID 118443, 2020.

[8] S. R. Obireddy and W.-F. Lai, "ROS-generating amine-functionalized magnetic nanoparticles coupled with carboxymethyl chitosan for pH-responsive release of doxorubicin," *International Journal of Nanomedicine*, vol. 17, pp. 589–601, 2022.

[9] M. Khatami, H. Q. Alijani, B. Fakheri et al., "Super-paramagnetic iron oxide nanoparticles (SPIONs): greener synthesis using *Stevia* plant and evaluation of its antioxidant properties," *Journal of Cleaner Production*, vol. 208, pp. 1171–1177, 2019.

[10] M. Szekeres, I. Y. Tóth, E. Illés et al., "Chemical and colloidal stability of carboxylated core–shell magnetite nanoparticles designed for biomedical applications," *International Journal of Molecular Sciences*, vol. 14, no. 7, pp. 14550–14574, 2013.

[11] A. V. Samrot, N. Shobana, P. Durga Sruthi, and C. S. Sahithya, "Utilization of chitosan-coated superparamagnetic iron oxide nanoparticles for chromium removal," *Applied Water Science*, vol. 8, Article ID 192, 2018.

[12] A. V. Samrot, P. Suresh, D. Rajalakshmi et al., "Superparamagnetic Iron Oxide Nanoparticles (SPIONs) as antibacterial agent and for Biomedical applications," *Journal of Pharmceutical Negative Results*, vol. 13, no. 9, pp. 713–718, 2022.

[13] S. Kayal and R. V. Ramanujan, "Doxorubicin loaded PVA coated iron oxide nanoparticles for targeted drug delivery," *Materials Science and Engineering: C*, vol. 30, no. 3, pp. 484–490, 2010.

[14] T. Lam, P. K. Avti, P. Pouliot et al., "Fabricating water dispersible superparamagnetic iron oxide nanoparticles for biomedical applications through ligand exchange and direct conjugation," *Nanomaterials*, vol. 6, no. 6, Article ID 100, 2016.

[15] A. V. Samrot, M. Sathiyasree, S. B. A. Rahim et al., "Scaffold using chitosan, agarose, cellulose, dextran and protein for tissue engineering—a review," *Polymers*, vol. 15, no. 6, Article ID 1525, 2023.

[16] P. Thevenot, S. Sohaebuddin, N. Poudyal, J. P. Liu, and L. Tang, "Magnetic nanoparticles to enhance cell seeding and distribution in tissue engineering scaffolds," in *2008 8th IEEE Conference on Nanotechnology*, pp. 646–649, IEEE, Arlington, TX, USA, August 2008.

[17] J. R. McCarthy and R. Weissleder, "Multifunctional magnetic nanoparticles for targeted imaging and therapy," *Advanced Drug Delivery Reviews*, vol. 60, no. 11, pp. 1241–1251, 2008.

[18] G. Huang, H. Chen, Y. Dong et al., "Superparamagnetic iron oxide nanoparticles: amplifying ROS stress to improve anticancer drug efficacy," *Theranostics*, vol. 3, no. 2, pp. 116–126, 2013.

[19] N. Schleich, P. Sibret, P. Danhier et al., "Dual anticancer drug/superparamagnetic iron oxide-loaded PLGA-based nanoparticles for cancer therapy and magnetic resonance imaging," *International Journal of Pharmaceutics*, vol. 447, no. 1-2, pp. 94–101, 2013.

[20] P.-E. Le Renard, R. Lortz, C. Senatore et al., "Magnetic and *in vitro* heating properties of implants formed *in situ* from injectable formulations and containing superparamagnetic iron oxide nanoparticles (SPIONs) embedded in silica microparticles for magnetically induced local hyperthermia," *Journal of Magnetism and Magnetic Materials*, vol. 323, no. 8, pp. 1054–1063, 2011.

[21] Y.-H. Choi, T. Yi, and D.-K. Kim, "Electron spin resonance (ESR) and microwave absorption studies of superparamagnetic iron oxide nanoparticles (SPIONs) for hyperthermia applications," *Journal of the Korean Ceramic Society*, vol. 48, no. 6, Article ID 577, 2011.

[22] S. Ruta, R. Chantrell, and O. Hovorka, "Unified model of hyperthermia via hysteresis heating in systems of interacting magnetic nanoparticles," *Scientific Reports*, vol. 5, Article ID 9090, 2015.

[23] S. R. Mousavi, M. Asghari, and N. M. Mahmoodi, "Chitosan-wrapped multiwalled carbon nanotube as filler within PEBA thin film nanocomposite (TFN) membrane to improve dye removal," *Carbohydrate Polymers*, vol. 237, Article ID 116128, 2020.

[24] M. Oveisi, M. A. Asli, and N. M. Mahmoodi, "Carbon nanotube based metal–organic framework nanocomposites: synthesis and their photocatalytic activity for decolorization of colored wastewater," *Inorganica Chimica Acta*, vol. 487, pp. 169–176, 2019.

[25] A. Almasian, M. E. Olya, and N. M. Mahmoodi, "Preparation and adsorption behavior of diethylenetriamine/polyacrylonitrile composite nanofibers for a direct dye removal," *Fibers and Polymers*, vol. 16, pp. 1925–1934, 2015.

[26] N. M. Mahmoodi, M. Oveisi, M. Bakhtiari et al., "Environmentally friendly ultrasound-assisted synthesis of magnetic zeolitic imidazolate framework–graphene oxide nanocomposites and pollutant removal from water," *Journal of Molecular Liquids*, vol. 282, pp. 115–130, 2019.

[27] N. M. Mahmoodi, A. Taghizadeh, M. Taghizadeh, and M. A. S. Baglou, "Surface modified montmorillonite with cationic surfactants: preparation, characterization, and dye adsorption from aqueous solution," *Journal of Environmental Chemical Engineering*, vol. 7, no. 4, Article ID 103243, 2019.

[28] N. M. Mahmoodi, M. Bashiri, and S. J. Moeen, "Synthesis of nickel–zinc ferrite magnetic nanoparticle and dye degradation using photocatalytic ozonation," *Materials Research Bulletin*, vol. 47, no. 12, pp. 4403–4408, 2012.

[29] A. V. Samrot, R. Sanjay Preeth, P. Prakash et al., "Extraction of fibres from *Cucumis melo* seed coat and its application as biosorbents for the effective removal of various dyes and antibiotic," *Biomass Conversion and Biorefinery*, 2022.

[30] P. Xu, G. M. Zeng, D. L. Huang et al., "Use of iron oxide nanomaterials in wastewater treatment: a review," *Science of the Total Environment*, vol. 424, pp. 1–10, 2012.

[31] S. Laurent, A. A. Saei, S. Behzadi, A. Panahifar, and M. Mahmoudi, "Superparamagnetic iron oxide nanoparticles for delivery of therapeutic agents: opportunities and challenges," *Expert Opinion on Drug Delivery*, vol. 11, no. 9, pp. 1449–1470, 2014.

[32] H. Mok and M. Zhang, "Superparamagnetic iron oxide nanoparticle-based delivery systems for biotherapeutics," *Expert Opinion on Drug Delivery*, vol. 10, no. 1, pp. 73–87, 2013.

[33] C. Janko, T. Ratschker, K. Nguyen et al., "Functionalized superparamagnetic iron oxide nanoparticles (SPIONs) as platform for the targeted multimodal tumor therapy," *Frontiers in Oncology*, vol. 9, Article ID 59, 2019.

[34] S. H. Crayton, A. K. Chen, J. F. Liu et al., "3.20 molecular imaging," in *Comprehensive Biomaterials*, vol. 3, pp. 424–466, Elsevier, 2017.

[35] C. Justin, S. A. Philip, and A. V. Samrot, "Synthesis and characterization of superparamagnetic iron-oxide nanoparticles (SPIONs) and utilization of SPIONs in X-ray imaging," *Applied Nanoscience*, vol. 7, pp. 463–475, 2017.

[36] A. V. Samrot, N. Shobana, M. Sathiyasree et al., "Toxicity evaluation of SPIONs on *Danio rerio* embryonic development," *Materials Today: Proceedings*, vol. 59, Part 2, pp. 1555–1560, 2022.

[37] B. Szalay, E. Tátrai, G. Nyírő, T. Vezér, and G. Dura, "Potential toxic effects of iron oxide nanoparticles in *in vivo* and *in vitro* experiments," *Journal of Applied Toxicology*, vol. 32, no. 6, pp. 446–453, 2012.

[38] A. V. Samrot, S. P. R. Singh, R. Deenadhayalan, V. V. Rajesh, S. Padmanaban, and K. Radhakrishnan, "Nanoparticles, a double-edged sword with oxidant as well as antioxidant properties—a review," *Oxygen*, vol. 2, no. 4, pp. 591–604, 2022.

[39] U. S. Gaharwar and R. Paulraj, "Iron oxide nanoparticles induced oxidative damage in peripheral blood cells of rat," *Journal of Biomedical Science and Engineering*, vol. 8, no. 4, pp. 274–286, 2015.

[40] M. Horie and Y. Tabei, "Role of oxidative stress in nanoparticles toxicity," *Free Radical Research*, vol. 55, no. 4, pp. 331–342, 2021.

[41] N. Shobana, P. Prakash, A. V. Samrot et al., "Evaluation of the toxic effect of *Bauhinia purpurea* mediated synthesized silver nanoparticles against *In-vitro* and *In-vivo* models," *Toxics*, vol. 11, no. 1, Article ID 9, 2023.

[42] R. Vakili-Ghartavol, A. A. Momtazi-Borojeni, Z. Vakili-Ghartavol et al., "Toxicity assessment of superparamagnetic iron oxide nanoparticles in different tissues," *Artificial Cells, Nanomedicine, and Biotechnology*, vol. 48, no. 1, pp. 443–451, 2020.

[43] S. Sharifi, S. Behzadi, S. Laurent, M. Laird Forrest, P. Stroeve, and M. Mahmoudi, "Toxicity of nanomaterials," *Chemical Society Reviews*, vol. 41, no. 6, pp. 2323–2343, 2012.

[44] N. M. Dissanayak, K. M. Current, and S. O. Obare, "Mutagenic effects of iron oxide nanoparticles on biological cells," *International Journal of Molecular Sciences*, vol. 16, no. 10, pp. 23482–23516, 2015.

[45] Y. Totsuka, K. Ishino, T. Kato et al., "Magnetite nanoparticles induce genotoxicity in the lungs of mice via inflammatory response," *Nanomaterials*, vol. 4, no. 1, pp. 175–188, 2014.

[46] M. B. Radu, I. M. P. Din, A. Hermenea et al., "Exposure to iron oxide nanoparticles coated with phospholipid-based polymeric micelles induces biochemical and histopathological pulmonary changes in mice," *International Journal of Molecular Sciences*, vol. 16, no. 12, pp. 29417–29435, 2015.

[47] I. Iavicoli, L. Fontana, V. Leso, and A. Bergamaschi, "The effects of nanomaterials as endocrine disruptors," *International Journal of Molecular Sciences*, vol. 14, no. 8, pp. 16732–16801, 2013.

[48] A. Awaad, "Histopathological and immunological changes induced by magnetite nanoparticles in the spleen, liver and genital tract of mice following intravaginal instillation," *The Journal of Basic & Applied Zoology*, vol. 71, pp. 32–47, 2015.

[49] M.-Q. Zhang, B. Chen, J.-P. Zhang, N. Chen, C.-Z. Liu, and C.-Q. Hu, "Liver toxicity of macrolide antibiotics in zebrafish," *Toxicology*, vol. 441, Article ID 152501, 2020.

[50] S. A. Reinecke and A. J. Reinecke, "The comet assay as biomarker of heavy metal genotoxicity in earthworms," *Archives of Environmental Contamination and Toxicology*, vol. 46, pp. 208–215, 2004.

[51] W. J. Yang, J. H. Lee, S. C. Hong, J. Lee, J. Lee, and D.-W. Han, "Difference between toxicities of iron oxide magnetic nanoparticles with various surface-functional groups against human normal fibroblasts and fibrosarcoma cells," *Materials*, vol. 6, no. 10, pp. 4689–4706, 2013.

[52] A. V. Samrot, C. Justin, S. Padmanaban, and U. Burman, "A study on the effect of chemically synthesized magnetite nanoparticles on earthworm: *Eudrilus eugeniae*," *Applied Nanoscience*, vol. 7, pp. 17–23, 2017.

[53] A. S. Remya, M. Ramesh, M. Saravanan, R. K. Poopal, S. Bharathi, and D. Nataraj, "Iron oxide nanoparticles to an Indian major carp, *Labeo rohita*: impacts on hematology, iono regulation and gill Na^+/K^+ ATPase activity," *Journal of King Saud University—Science*, vol. 27, no. 2, pp. 151–160, 2015.

[54] S. Karthikeyeni, T. Siva Vijayakumar, S. Vasanth, A. Ganesh, M. Manimegalai, and P. Subramanian, "Biosynthesis of iron oxide nanoparticles and its haematological effects on fresh water fish *Oreochromis mossambicus*," *Journal of Academia and Industrial Research*, vol. 1, no. 10, pp. 645–649, 2013.

[55] M. Saravanan, R. Suganya, M. Ramesh, R. K. Poopal, N. Gopalan, and N. Ponpandian, "Iron oxide nanoparticles induced alterations in haematological, biochemical and ionoregulatory responses of an Indian major carp *Labeo rohita*," *Journal of Nanoparticle Research*, vol. 17, Article ID 274, 2015.

[56] A. V. Samrot, M. Bavanilatha, S. K. Shree et al., "Evaluation of heavy metal removal of nanoparticles based adsorbent using *Danio rerio* as model," *Toxics*, vol. 10, no. 12, Article ID 742, 2022.

[57] N. Shobana, P. Prakash, A. V. Samrot et al., "Nanotoxicity studies of *Azadirachta indica* mediated silver nanoparticles against *Eudrilus eugeniae*, *Danio rerio* and its embryos," *Biocatalysis and Agricultural Biotechnology*, vol. 47, Article ID 102561, 2023.

[58] L. Lei, J. Ling-Ling, Z. Yun, and L. Gang, "Toxicity of superparamagnetic iron oxide nanoparticles: research strategies and implications for nano medicine," *Chinese Physics B*, vol. 22, no. 12, Article ID 127503, 2013.

[59] A. V. Samrot, C. SaiPriya, J. Lavanya Agnes Angalene et al., "Evaluation of nanotoxicity of *Araucaria heterophylla* gum derived green synthesized silver nanoparticles on *Eudrilus eugeniae* and *Danio rerio*," *Journal of Cluster Science*, vol. 30, pp. 1017–1024, 2019.

[60] R. D. Cardiff, C. H. Miller, and R. J. Munn, "Manual hematoxylin and eosin staining of mouse tissue sections," *Cold Spring Harbor Protocols*, vol. 2, no. 6, pp. 655–658, 2014.

[61] D. C. Sheehan and B. B. Hrapchak, *Theory and Practice of Histotechnology*, Battelle Press, Ohio, 2nd edition, 1980.

[62] L. G. Luna, *Manual of Histologic Staining Methods of the AFIP*, McGraw-Hill, NY, 3rd edition, 1968.

[63] J. N. Crookham and R. W. Dapson, *Hazardous Chemicals in the Histopathology Laboratory*, ANATECH, 2nd edition, 1991.

[64] A. V. Samrot, C. S. Sahithya, S. P. Durga et al., "Itraconazole coated super paramagnetic iron oxide nanoparticles for antimicrobial studies," *Biointerface Research in Applied Chemistry*, vol. 10, no. 5, pp. 6218–6225, 2020.

[65] A. V. Samrot, C. S. Sahithya, J. A. Selvarani, S. Pachiyappan, and S. S. Kumar, "Surface-engineered super-paramagnetic iron oxide nanoparticles for chromium removal," *International Journal of Nanomedicine*, vol. 14, pp. 8105–8119, 2019.

[66] A. V. Samrot, U. Burman, S. Padmanaban, P. Yamini, and A. M. Rabel, "A study on toxicity of chemically synthesised silver nanoparticle on *Eudrilus eugeniae*," *Toxicology and Environmental Health Sciences*, vol. 10, pp. 162–167, 2018.

[67] K. Sathya, R. Saravanathamizhan, and G. Baskar, "Ultrasound assisted phytosynthesis of iron oxide nanoparticle," *Ultrasonics Sonochemistry*, vol. 39, pp. 446–451, 2017.

[68] S. Shukla, A. Jadaun, V. Arora, R. K. Sinha, N. Biyani, and V. K. Jain, "*In vitro* toxicity assessment of chitosan

oligosaccharide coated iron oxide nanoparticles," *Toxicology Reports*, vol. 2, pp. 27–39, 2015.

[69] A. H. Fischer, K. A. Jacobson, J. Rose, and R. Zeller, "Hematoxylin and eosin staining of tissue and cell sections," *Cold Spring Harbor Protocols*, 2008.

[70] K. Rowatt, R. E. Burns, S. Frasca Jr., and D. M. Long, "A combination Prussian blue—hematoxylin and eosin staining technique for identification of iron and other histological features," *Journal of Histotechnology*, vol. 41, no. 1, pp. 29–34, 2018.

[71] R. A. R. Villacis, J. S. Filho, B. Piña et al., "Integrated assessment of toxic effects of maghemite (γ-Fe_2O_3) nanoparticles in zebrafish," *Aquatic Toxicology*, vol. 191, pp. 219–225, 2017.

[72] M. F. Valerio-Rodríguez, L. I. Trejo-Téllez, M. A. Aguilar-González et al., "Effects of ZnO, TiO_2 or Fe_2O_3 nanoparticles on the body mass, reproduction, and survival of *Eisenia fetida*," *Polish Journal of Environmental Studies*, vol. 29, no. 3, pp. 2383–2394, 2020.

[73] C. Chakraborty, A. R. Sharma, G. Sharma, and S.-S. Lee, "Zebrafish: a complete animal model to enumerate the nanoparticle toxicity," *Journal of Nanobiotechnology*, vol. 14, Article ID 65, 2016.

[74] A. Raj, P. Shah, and N. Agrawal, "Sedentary behavior and altered metabolic activity by AgNPs ingestion in *Drosophila melanogaster*," *Scientific Reports*, vol. 7, Article ID 15617, 2017.

[75] C. Ong, L.-Y. Lanry Yung, Y. Cai, B.-H. Bay, and G.-H. Baeg, "*Drosophila melanogaster* as a model organism to study nanotoxicity," *Nanotoxicology*, vol. 9, no. 3, pp. 396–403, 2015.

[76] A. V. Samrot, C. SaiPriya, S. A. Jenifer et al., "A study on influence of superparamagnetic iron oxide nanoparticles (SPIONs) on green gram (*Vigna radiata* L.) and earthworm (*Eudrilus eugeniae* L.)," *Materials Research Express*, vol. 7, no. 5, Article ID 055002, 2020.